J. Chem. Thermodynamics 138 (2019) 151–158

Contents lists available at ScienceDirect

J. Chem. Thermodynamics

journal homepage: www.elsevier.com/locate/jct

Thermodynamic interpretation of uranium(IV/VI) solubility in the presence of α-isosaccharinic acid

Taishi Kobayashi [a,*], Takayuki Sasaki [a], Akira Kitamura [b]

[a] Department of Nuclear Engineering, Kyoto University, Kyotodaigaku-katsura, Nishikyo-ku, Kyoto 615-8540, Japan
[b] Radionuclide Migration Research Group, Sector of Nuclear Fuel, Decommissioning and Waste Management Technology Development, Japan Atomic Energy Agency, Tokai, Ibaraki 319-1194, Japan

ARTICLE INFO

Article history:
Received 23 May 2019
Accepted 6 June 2019
Available online 10 June 2019

Keywords:
Uranium(IV)
Uranium(VI)
Solubility
Isosaccharinate
Complex formation

ABSTRACT

The effect of α-isosaccharinic acid (ISA) on the solubility and redox of tetravalent and hexavalent uranium (U(IV), U(VI)) was investigated in the hydrogen ion concentration ($pH_c = -\log [H^+]$) range of 6–13 and at total ISA concentration ($[ISA]_{tot}$) = 10^{-4}–$10^{-1.2}$ mol/dm^3 (M). The dependence of U(IV) solubility on pH_c and $[ISA]_{tot}$ suggested the existence of $U(OH)_4(ISA)_2^{2-}$ as a dominant species within the investigated pH_c range of 6–12. For the U(VI)-ISA system, $UO_2(OH)_3(ISA)_2^{3-}$ was suggested as a dominant species at pH_c 7–13. The formation constants of the U(IV)-ISA and U(VI)-ISA complexes were determined by least squares fitting of the solubility data. The solubility of U(IV) and U(VI) in the presence of ISA and its effect on the redox behavior were thermodynamically interpreted based on the obtained constants.

© 2019 Elsevier Ltd.

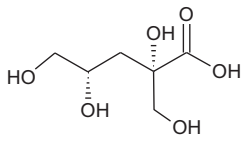
1. Introduction

The safety assessment of geological disposal of high-level radioactive waste and TRU waste (low-level waste generated after reprocessing spent nuclear fuels and fabrication of MOX fuels) requires the solubility limit prediction of radionuclides under relevant repository conditions. Cellulosic materials contained in low-level (and intermediate-level for some countries) wastes degrade to smaller organic substances under cementitious alkaline conditions and α-isosaccharinic acid (ISA) is known as a primary degradation product [1,2]. ISA is a poly-hydroxy-carboxylic acid with a terminal carboxylic group and four alcoholic groups on the primary and side chains (Fig. 1). Owing to the formation of stable complexes with metal ions, ISA has been considered to potentially enhance the solubility of radionuclides, which could affect the safety assessment of TRU waste disposal. The interaction of ISA with radionuclides including long-lived actinide elements has been reviewed as a part of Thermochemical Database Project organized by the Nuclear Energy Agency in Organisation for Economic Cooperation and Development (NEA-TDB) [3]. Although several researchers have investigated the interaction between metal ions and ISA, the number of reported values of thermodynamic constant such as the complex formation constant was considerably limited for some actinide elements [4–10]. Uranium is one of the elements, on which few studies have proposed the dominant ISA complexes and their formation constants [4,8,11,12].

Under reducing geochemical conditions in the repository system, the tetravalent state (U(IV)) is the most relevant oxidation state for uranium. Owing to the strong hydrolysis reaction, U(IV) precipitates easily as a sparingly soluble amorphous hydroxide ($U(OH)_4$(am)) or hydrous oxide (UO_2(am, hyd)) in the neutral to alkaline pH range [13–15]. The formation of the soluble U(IV)-ISA complex potentially increases the apparent solubility of uranium, which can mobilize uranium in the repository system. However, the influence of ISA on U(IV) solubility has been investigated in two studies [4,11] and only Warwick et al. [11] has reported the formation constant (β) of U(IV)-ISA. The U(IV) solubility was measured at pH 3.2, 6.2, and 13.5 in the presence of 0.0444 and 0.0615 mol/dm^3 (M) ISA and the formation constant of $U(OH)_4(ISA)^-$ was determined as log β ($U(OH)_4(ISA)^-$) = 49 [11]. However, the investigated experimental conditions remained in the limited number of plots and narrow ranges of pH and ISA concentration. Gaona et al. [8] have recently reviewed literature studies on the complexation of ISA and tetravalent actinides (An(IV)). Based on the linear free-energy relationship between the experimentally determined complexation constants of ISA with other An(IV), the constants of $U(OH)_4(ISA)^-$ and $U(OH)_4(ISA)_2^{2-}$ were estimated to be log β ($U(OH)_4(ISA)^-$) = 49.2 ± 0.9 and log β ($U(OH)_4(ISA)_2^{2-}$) = 51.1 ± 1.0 [8], respectively. As described above, owing to the poor experimental data on the U(IV)-ISA complexation, the speciation and thermodynamic constant are still unclear.

* Corresponding author.
E-mail address: kobayashi@nucleng.kyoto-u.ac.jp (T. Kobayashi).

https://doi.org/10.1016/j.jct.2019.06.006
0021-9614/© 2019 Elsevier Ltd.



HISA

Fig. 1. Chemical formula of α-isosaccharinic acid (HISA).

The hexavalent oxidation state (U(VI)) may be relevant under the occasional oxidizing condition in the repository system. Rao et al. [12] examined the complex formation of U(VI)-ISA based on potentiometric and calorimetric measurements and determined the constants for binary complexes of $UO_2(ISA)^{2+}$, $UO_2(ISA)_2(aq)$, and $UO_2(ISA)_3^-$. In their experiments, the pH range was limited to the acidic pH region to avoid the precipitation of U(VI); thus, the U(VI)-ISA species dominant in the neutral to alkaline pH range is unclear. The formation of stable U(VI)-ISA species possibly affects the redox behavior of uranium in the repository system.

In the present study, we focused on the solubilities of U(IV) and U(VI) in the presence of ISA at hydrogen ion concentrations ($pH_c = -\log [H^+]$) of 6–13 and total concentration of ISA ($[ISA]_{tot}$) of 10^{-4}–$10^{-1.2}$ M. Based on the solid-phase analysis and slope analysis of the solubilities, dominant U(IV)-ISA and U(VI)-ISA complexes were revealed and their formation constants were determined by the thermodynamic analysis of the solubility data. The effect of ISA on the solubility and redox behavior of uranium was described by the obtained constants.

2. Experimental

2.1. Materials and reagents

All chemicals used were of reagent grade. Sodium chloride (NaCl), sodium dithionite ($Na_2S_2O_4$), hydrochloric acid (HCl), sodium carbonate (Na_2CO_3) and a standard solution of carbonate-free sodium hydroxide (NaOH) were purchased from Wako Pure Chem. Deionized purified water (Milli-Q, Millipore) was used in all solution preparations and purged for several hours with argon gas before use. Calcium alpha-D-isosaccharinate ($C_{12}H_{22}CaO_{12}$; $Ca(ISA)_2$) was prepared using the method reported by Whistler and BeMiller [16] from α–lactose (Wako Pure Chem.) and characterized by X-ray diffraction (XRD) elsewhere [17]. Elemental analysis calculated for $C_{12}H_{22}O_{12}Ca$: C 36.18, H 5.57% was found to be C 34.49, H 5.63%. A stock solution of 0.5 M sodium isosaccharinate (NaISA) was subsequently prepared from $Ca(ISA)_2$ using the method described in the literature [7]. A 2.16 g portion of $Ca(ISA)_2$ was reacted overnight with 16 mL of 0.5 M Na_2CO_3 in 0.01 M NaOH solution to precipitate Ca as $CaCO_3$, resulting NaISA in aqueous phase. The aqueous phase was then separated from $CaCO_3$ by centrifugation. A table of all chemicals and compounds used in the present study is given in Table A1 as Supporting Information.

All sample preparation and handling were performed in an Ar-glove box at T = 25 °C with an O_2 concentration below 10 ppm and under carbonate exclusion. A combined glass electrode (9615-10D, Horiba Ltd.) was used to measure the pH_c. The reference electrode was filled with 3.6 M NaCl and 0.4 M $NaClO_4$ (Wako Pure Chem.). The electrode was calibrated against standard HCl and NaOH solutions (pH_c 1, 2, 3, 11, 12, and 13; Wako Pure Chem.) at ionic strength (I) = 0.5 M by NaCl to correct the experimentally measured pH_{exp} values to the pH_c values. The redox potential in solution was determined with a Pt combination electrode (9300-10D, Horiba Ltd.) equipped with an Ag/AgCl reference system. The measured redox potential value was recorded after several minutes and converted into E_h (redox potential vs. standard hydrogen electrode) by adding the Ag/AgCl reference electrode potential (+208 mV for 3 M KCl junction electrolyte). The apparent electron activity ($pe = -\log a_{e^-}$) was calculated from $E_h = -(RT/F) \ln a_{e^-}$ according to the relation $pe = 16.9\ E_h$ (V) at 25 °C.

2.2. Sample preparation

2.2.1. Preparation for U(IV)-ISA samples

Uranyl nitrate hexahydrate ($UO_2(NO_3)_2{\cdot}6H_2O$, Nakalai) was dissolved in 0.1 M nitric acid (HNO_3) to obtain 50 mL of 0.06 M U(VI) stock solution. The U(VI) stock solution was subsequently reduced electrochemically at −1.0 V for 3 h using an electrochemical analyzer (BAS, ALS611E). By measuring the ultraviolet–visible (UV–Vis) spectra (BAS, SEC2000) of the solution, the initial U(VI) was confirmed to be completely reduced to U(IV). Portions of concentrated NaOH solution was subsequently added into the U(IV) stock solution to precipitate amorphous U(IV) hydrous oxide (UO_2(am, hyd)). The precipitate was washed several times with a 1 mM $Na_2S_2O_4$ solution to avoid any oxidation and finally suspended in 20 mL of 1 mM $Na_2S_2O_4$ solution at pH_c of ∼10. The U(IV) concentration corresponded to ∼0.15 M when the precipitate was completely dissolved.

Sample solutions at specific pH_c and $[ISA]_{tot}$ were prepared by an undersaturation method. Before adding a portion of the suspended stock solution of UO_2(am, hyd) to each sample tube, the pH_c was adjusted to 6–12 using HCl/NaOH and the $[ISA]_{tot}$ was adjusted to 10^{-3}–$10^{-1.2}$ M by the appropriate amount of NaISA stock solution. The ionic strength (I) of each sample solution was set to 0.5 using the 5 M NaCl stock solution. The sample solutions deposited in polypropylene tubes were placed in glass bottles and stored in an Ar glove box to avoid the oxidation of U(IV) during the solubility experiment. The sample tubes were shaken by hand occasionally for a few minutes during the aging process up to 75 days (d).

2.2.2. Preparation of U(VI)-ISA samples

A stock solution of 0.33 M U(VI) was prepared by dissolving $UO_2(NO_3)_2{\cdot}6H_2O$ in 0.1 M HNO_3. Portions of concentrated NaOH solution were subsequently added rapidly into the U(VI) stock solution to obtain U(VI) precipitates at a pH_c of ∼10. The precipitates were subsequently washed with purified water several times to obtain a 40 mL stock suspension of U(VI) precipitate. The U(VI) concentration corresponded to ∼0.3 M when the precipitate was completely dissolved. A portion of U(VI) precipitate was stored for ∼10 weeks and confirmed to be $Na_2U_2O_7{\cdot}H_2O$(cr) (JCPDS file 871714) by its X-ray diffraction pattern (RINT200, RIGAKU) measurement.

Sample solutions at specific pH_c and $[ISA]_{tot}$ were prepared by an undersaturation method. Before adding the U(VI) precipitate to each sample tube, the pH_c and $[ISA]_{tot}$ were adjusted in the ranges of 7–13 and 10^{-4}–$10^{-1.2}$ M, respectively, by adding the appropriate amount of HCl/NaOH and NaISA stock solution. The ionic strength of each sample solution was set to I = 0.5 using 5 M NaCl stock solution. To confirm the U(VI) solubility in the absence of ISA, several samples without adding ISA were prepared similarly. The sample tubes were stored in an Ar glove box to avoid the contamination of CO_2 in the air. They were shaken by hand occasionally for a few minutes during the aging process up to 123 d.

2.3. Solubility measurements

After aging for a given period, the pH_c of the U(IV)-ISA and U(VI)-ISA samples was measured. For the U(IV)-ISA samples, the E_h

values were measured to confirm that the reducing condition was maintained during the aging time. Each 0.5 mL of the supernatant of the sample solution was subsequently filtrated through an ultrafiltration membrane (Microcon, nominal molecular weight limit (NMWL) of 10^4 (10 kDa), corresponding to pore sizes of approximately 3 nm, Millipore). The filtrate was acidified with nitric acid and diluted in 0.1 M HNO_3 for the measurement by ICP-MS (inductively coupled plasma mass spectrometry) with a PlasmaQuant MS Elite (Jena Analytik). The detection limit of U(IV) and U(VI) solubility corresponded to $\sim 10^{-8}$ M. The solubility measurement was repeated several times to confirm that the solubility reaction reached the steady state. The standard error was within 10% for each measurement by ICP-MS, which resulted in ± 0.1 in the log unit of uranium concentration. For selected samples, the solid phase was separated by centrifugation after the solubility measurement and dried at room temperature to collect their X-ray diffraction patterns (RINT200, RIGAKU).

3. Results and discussion

3.1. Solubility of uranium(IV) in the presence of ISA

The experimentally measured pH_c and pe values of the sample solutions are shown in Table A2 in Appendix A. The pH_c and pe values buffered by $Na_2S_2O_4$ were generally maintained under reducing conditions, where the U(IV) solid phase and soluble species were considered dominant. Fig. 2 shows the U(IV) solubility in the presence of $10^{-2.7}$, $10^{-2.1}$, and $10^{-1.5}$ M ISA after ultrafiltration through 10 kDa membranes as a function of pH_c, over an aging period of 24–75 d. The solubility of $UO_2{\cdot}xH_2O$(am) and/or $U(OH)_4$(am) in the absence ISA has been measured in a neutral to alkaline pH range [18–20], and those reported in the range of pH_c 6–12 [19] are plotted in Fig. 2 as a comparison. As the solubility data after 24 d indicated stable values, a steady state between the solution species and solid phase was considered to be achieved within several weeks. In the presence of $10^{-2.7}$ M ISA, the solubility was comparable to that without ISA, indicating the limited effect of ISA on U(IV) solubility. In the presence of $10^{-2.1}$ and $10^{-1.5}$ M ISA, the obtained values increased with the ISA concentration, indicating the formation of the U(IV)-ISA complex. At both $[ISA]_{tot}$, the U(IV) solubility was found to be almost constant against pH_c. If the solid phase was UO_2(am, hyd), it was suggested that four OH^- ions were involved in the U(IV)-ISA complex. In the system of tetravalent actinides (An(IV)) and Zr(IV), as an analog of An(IV), the solubilities of Th(IV), Np(IV), and Zr(IV) were measured in the presence of ISA [7,9,17]. For Th(IV) and Np(IV), the solubilities were observed to be independent of pH_c in the region of pH_c 8–12, and $An(OH)_4(ISA)_x$ (x = 1, 2) was proposed as the dominant species. A similar trend was observed in the Zr(IV) solubility in the range of pH_c 8–12. The Pu(IV) solubility in the presence of ISA has been investigated recently, where the Pu(IV) solubility was constant at pH_c < 12, although the solubility increased at pH_c > 12 [10]. These results support that An(IV) forms the ternary hydroxo-ISA complex of $An(OH)_4(ISA)_x$ at pH_c < 12, which significantly enhances the apparent An(IV) solubility in the neutral to alkaline pH condition.

In Fig 3, U(IV) solubilities at (a) pH_c = 6.8–7.6 and (b) pH_c = 9.5–10.6 were shown as a function of $[ISA]_{tot}$. The U(IV) solubilities increased with $[ISA]_{tot}$ with a slope of approximately two, indicating that two ISAs were involved in the U(IV)-ISA complex. At pH_c = 9.5–10.6 and $[ISA]_{tot}$ < 0.01 M, the slope was observed to be slightly deviated from two, thus suggesting a possible contribution of the U(IV)-ISA complex containing one ISA. A similar slope of the solubility against $[ISA]_{tot}$ was observed in Th(IV), Np(IV), and Zr(IV), resulting in the complexes of $An(OH)_4(ISA)^-$, $An(OH)_4(ISA)_2^{2-}$, and $Zr(OH)_4(ISA)_2^{2-}$ as dominant species under the neutral to alkaline pH condition [7,9,17].

Fig. 4 represents the XRD patterns of the U(IV) solid phase aged in the presence of $10^{-1.5}$ M ISA. In the XRD spectra of the solid phases at pH_c 7.0 and 10.5, only three peaks (31.6, 45.4, and 56.4°) corresponding to NaCl(cr) (JCPDS file 050628) used as an electrolyte in the investigated system were found, which might contaminate the sample during the separation process of the solid phase. As no additional peak corresponding to the U(IV) compounds was observed, it was suggested that the solid phases were not likely converted to another solid phase from the initial UO_2(am, hyd).

3.2. Solubility of uranium(VI) in the presence of ISA

The experimentally measured pH_c and pe values of the sample solutions are shown in Table A3 in Appendix A. Fig. 5 shows the

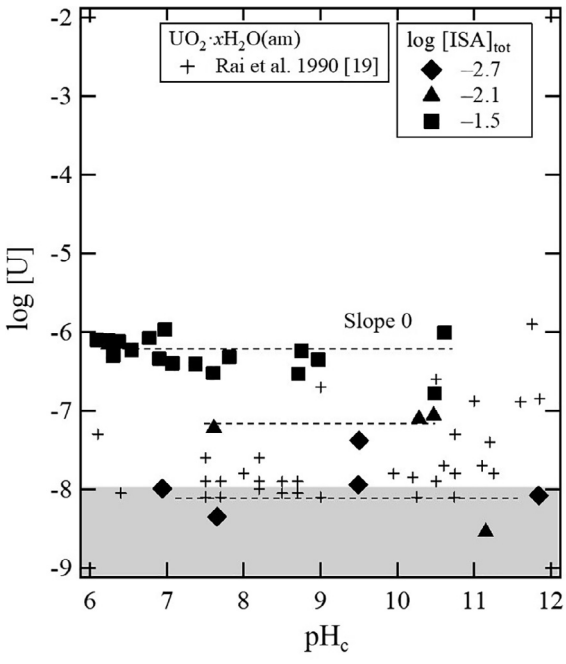


Fig. 2. U(IV) solubility in the presence of $10^{-2.7}$, $10^{-2.1}$, and $10^{-1.5}$ M ISA after aging for 24–75 d. The sample solutions were filtrated through 10-kDa membranes. The detection limit level of the ICP-MS was indicated by a gray field in the figure.

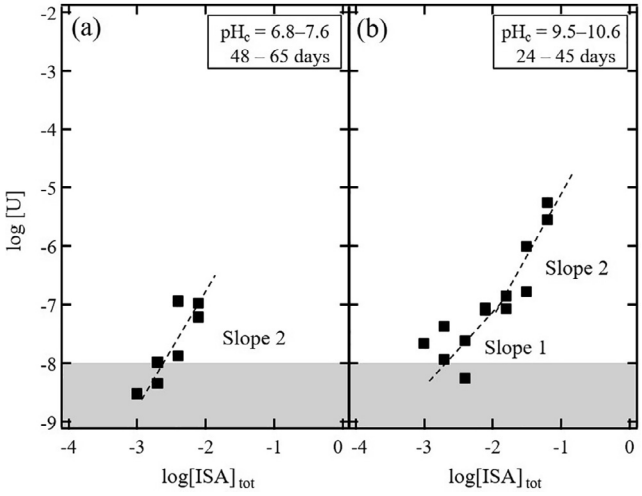


Fig. 3. U(IV) solubility at (a) pH_c = 6.8–7.6 and (b) pH_c = 9.5–10.6 after ultrafiltration through 10kDa membranes as a function of total ISA concentration. The detection limit level of the ICP-MS was indicated by a gray field in the figure.

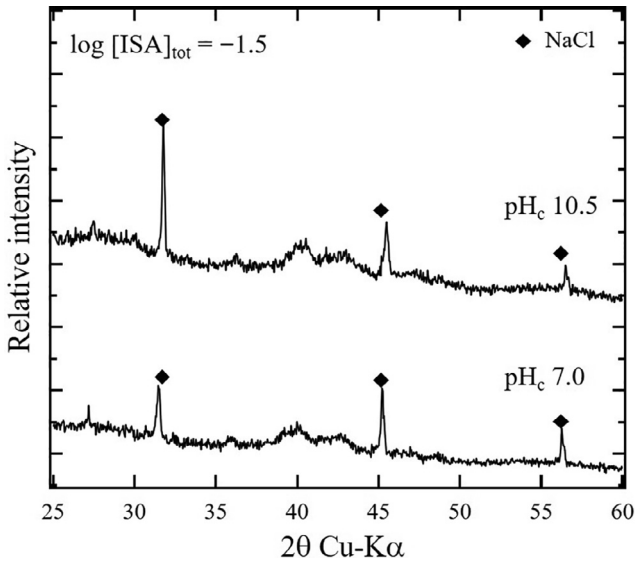


Fig. 4. XRD patterns of the U(IV) solid phase formed in the presence of $10^{-1.5}$ M ISA. The indicator (◆) represents the reference peak position of NaCl(cr) (JCPDS file 050628) used as an electrolyte in the experiment.

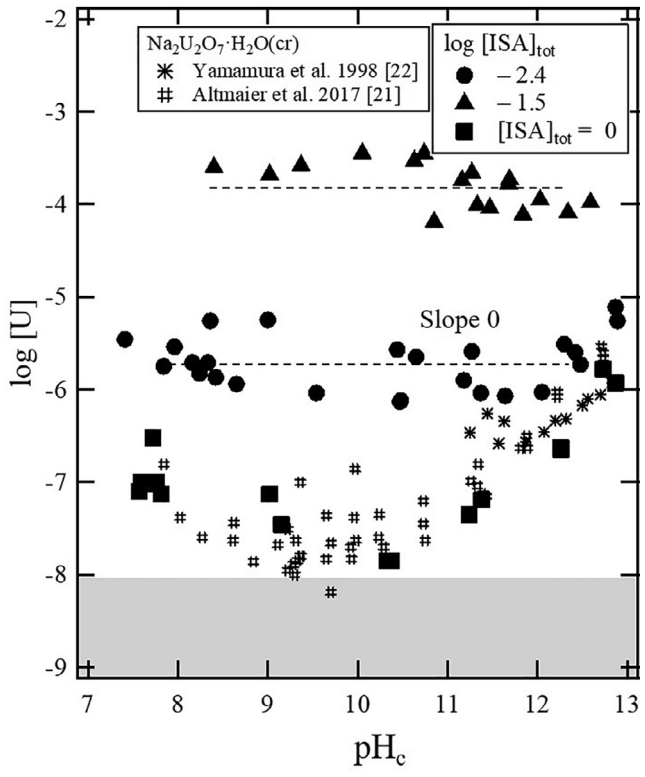


Fig. 5. U(VI) solubility in the absence and presence of $10^{-2.4}$ and $10^{-1.5}$ M ISA after aging for 19–123 d. The sample solutions were filtrated through 10 kDa membranes. The detection limit level of the ICP-MS was indicated by a gray field in the figure.

U(VI) solubility in the absence and presence of $10^{-2.4}$ and $10^{-1.5}$ M ISA after ultrafiltration through 10 kDa membranes as a function of pH_c, over an aging period of 19–123 d. The solubility of $Na_2U_2O_7{\cdot}H_2O$(cr) in the absence ISA [21,22] were plotted in the figure to represent the effect of ISA in the neutral to alkaline pH region. The solubility data after 19 d exhibited similar values, indicating that a steady state was achieved within a few weeks. In the absence of ISA, the solubility plots obtained in the present study are in good agreement with the literature values reported as the solubility of $Na_2U_2O_7{\cdot}H_2O$(cr) [21,22]. As described in the experiment, the initial solid phase without adding into the sample solution was confirmed to be $Na_2U_2O_7{\cdot}H_2O$(cr) through XRD spectra. The solubility in the absence of ISA also indicated that the solubility-limiting solid phase in this system was $Na_2U_2O_7{\cdot}H_2O$(cr).

In the presence of $10^{-2.4}$ M ISA, the solubility was approximately two orders of magnitude higher than those in the absence of ISA and almost constant around 10^{-6} M against pH in the investigated pH region of pH_c = 7–13. In the presence of $10^{-1.5}$ M ISA, the solubility was almost constant at $\sim 10^{-4}$ M regardless of pH in the investigated pH range. If the solid phase is $Na_2U_2O_7{\cdot}H_2O$ (cr), the slope of zero suggested that three OH^- ions were involved in the U(VI)-ISA complex.

Fig. 6 shows the U(VI) solubilities at (a) pH_c = 8.3–8.6, (b) pH_c = 10.3–10.8, and (c) pH_c = 12.0–12.3 as a function of total ISA concentration ($[ISA]_{tot}$). At each pH_c condition, the U(VI) solubility increased with the $[ISA]_{tot}$ with a slope of approximately two, indicating that two ISAs were involved in the U(VI)-ISA complex. The decrease in slope at $\log [ISA]_{tot} < -2$, pH_c = 12.0–12.3 was considered to be due to the increased contribution of the U(VI) hydrolysis species, $UO_2(OH)_4^{2-}$. In conjunction with the slope of U(VI) solubility against pH_c shown in Fig. 5, the dominant U(VI)-ISA species were considered to be $UO_2(OH)_3(ISA)_2^{3-}$ within the investigated pH_c and $[ISA]_{tot}$ ranges.

3.3. Thermodynamic model for uranium ISA system

3.3.1. Thermodynamic model for U(IV)-ISA

The solid phase aged in the presence of ISA was suggested to be UO_2(am, hyd) based on the XRD patterns of the precipitates. The U(IV) solubility was almost constant at pH_c = 6–12, indicating that the dominant species can be expressed as $U(OH)_4(ISA)_x$ in this pH region. The solubility increased with increasing $[ISA]_{tot}$ with a slope of two at pH_c = 6.8–7.6 and those of 1 and 2 at pH_c = 9.5–10.6, resulting in the possible formation of $U(OH)_4(ISA)^-$ and $U(OH)_4(ISA)_2^{2-}$. The equilibrium reactions for the solid phase and U(IV)-ISA complexes can be described below.

$$UO_2(am, hyd) + 2H_2O \rightleftharpoons U^{4+} + 4OH^- \quad (1)$$

$$\log K_{sp4} = \log [U^{4+}] + 4\log[OH^-], \quad (2)$$

$$U^{4+} + 4OH^- + ISA^- \rightleftharpoons U(OH)_4(ISA)^- \quad (3)$$

$$\log \beta_{141} = \log [U(OH)_4(ISA)^-] - \log \left[U^{4+}\right] - 4\log[OH^-] - \log [ISA^-], \quad (4)$$

$$U^{4+} + 4OH^- + 2ISA^- \rightleftharpoons U(OH)_4(ISA)_2^{2-} \quad (5)$$

$$\log \beta_{142} = \log \left[U(OH)_4(ISA)_2^{2-}\right] - \log \left[U^{4+}\right] - 4\log[OH^-] - 2\log [ISA^-], \quad (6)$$

In addition to the U(IV)-ISA complexes above, the hydrolysis species of $U(OH)_m^{(4-m)}$ was assumed in the analysis based on the NEA thermodynamic database [15]. Thus, the U(IV) solubility ([U(IV)]) can be described as follows:

$$[U(IV)] = \left[U^{4+}\right] + \sum_m \left[U(OH)_m^{(4-m)}\right] + [U(OH)_4(ISA)^-] + \left[U(OH)_4(ISA)_2^{2-}\right] \quad (7)$$

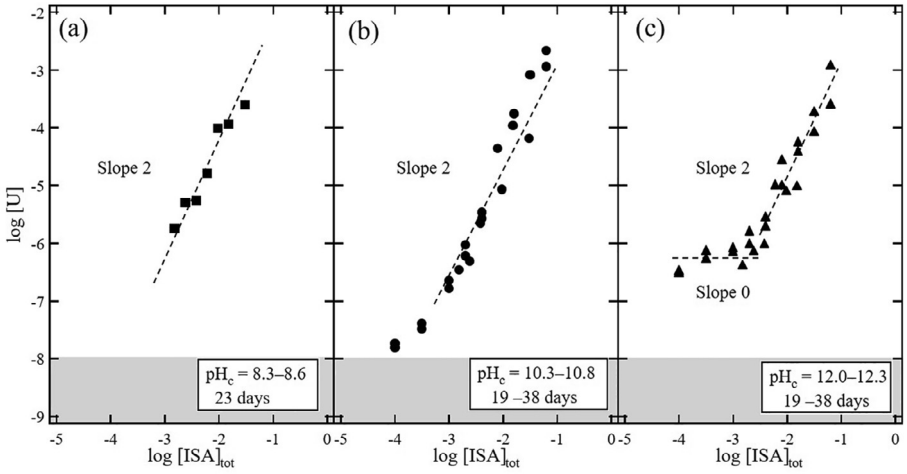


Fig. 6. U(VI) solubility at (a) pH_c = 8.3–8.6, (b) pH_c = 10.3–10.8, and (c) pH_c = 12.0–12.3 after ultrafiltration through 10 kDa membranes as a function of total ISA concentration. The detection limit level of the ICP-MS was indicated by a gray field in the figure.

Table 1
Summary of the thermodynamic constants in U(IV)-ISA system (I = 0).

Reactions	Values		Ref
UO_2(am, hyd) + $2H_2O \rightleftharpoons U^{4+} + 4OH^-$	log $K°_{sp4}$	−54.5	[15]
$U^{4+} + OH^- \rightleftharpoons UOH^{3+}$	log $\beta°_{110}$	13.46	[15]
$U^{4+} + 4OH^- \rightleftharpoons U(OH)_4$(aq)	log $\beta°_{140}$	46	[15]
$U^{4+} + 4OH^- + ISA^- \rightleftharpoons U(OH)_4(ISA)^-$	log $\beta°_{141}$	48.4 ± 0.4	Present study
$U^{4+} + 4OH^- + 2ISA^- \rightleftharpoons U(OH)_4(ISA)_2^{2-}$	log $\beta°_{142}$	50.6 ± 0.1	Present study

Using the U(IV)-ISA complex formation reactions, deprotonation of the carboxylic group of ISA, and lactonization of ISA (ISL) [23], the $[ISA]_{tot}$ can be written as a sum of the concentrations of ISA, protonated ISA (HISA), ISA^-, and the U(IV)-ISA complexes.

$$[ISA]_{tot} = [ISL] + [HISA] + [ISA^-] + 2\left[U(OH)_4(ISA)_2^{2-}\right] \quad (8)$$

It is noteworthy that because the investigated pH_c range was limited to pH_c > 6, the contributions of [HISA] and [ISL] to $[ISA]_{tot}$ was calculated to be negligible based on the pKa of HISA and the formation constant of ISL [23]. Moreover, considering that the $[ISA]_{tot}$ was significantly larger than the obtained U(IV) solubility, Eq. (8) was simplified as $[ISA]_{tot} = [ISA^-]$ in the present analysis. As the solubility experiment was conducted at I = 0.5, the thermodynamic constants shown in Eqs. (2)–(6) were used after an ionic strength correction by the specific ion interaction theory (SIT) [15]. Based on the SIT approach, the conditional complex formation constants (β_{141} and β_{142}) for $U(OH)_4(ISA)^-$ and $U(OH)_4(ISA)_2^{2-}$ can be described as

$$\begin{aligned}\log\beta_{141} &= \log\beta°_{141} + \log\gamma_{U(OH)^4(ISA)^-} - \left(\log\gamma_{U^{4+}} + 4\log\gamma_{OH^-} + \log\gamma_{ISA^-}\right)\\ &= \log\beta°_{141} - 20D - \left\{\varepsilon\left(U(OH)_4(ISA)^-, Na^+\right) - \varepsilon\left(U^{4+}, Cl^-\right)\right.\\ &\left. -4\varepsilon\left(OH^-, Na^+\right) - \varepsilon\left(ISA^-, Na^+\right)\right\}\cdot I_m\end{aligned} \quad (9)$$

$$\begin{aligned}\log\beta_{142} &= \log\beta°_{142} + \log\gamma_{U(OH)_4(ISA)_2^{2-}} - \left(\log\gamma_{U^{4+}} + 4\log\gamma_{OH^-} + 2\log\gamma_{ISA^-}\right)\\ &= \log\beta°_{142} - 18D\\ &\quad -\left\{\varepsilon\left(U(OH)_4(ISA)_2^{2-}, Na^+\right) - \varepsilon\left(U^{4+}, Cl^-\right)\right.\\ &\left. -4\varepsilon\left(OH^-, Na^+\right) - 2\varepsilon\left(ISA^-, Na^+\right)\right\}\cdot I_m,\end{aligned} \quad (10)$$

where $\beta°_{141}$ and $\beta°_{142}$ are the complex formation constants at I = 0. The ε ($U(OH)_4(ISA)^-$, Na^+), $\varepsilon(U(OH)_4(ISA)_2^{2-}, Na^+)$, $\varepsilon(U^{4+}, Cl^-)$, $\varepsilon(OH^-, Na^+)$, $\varepsilon(ISA^-, Na^+)$, and D represent the ion interaction coefficient for each species and the Debye–Hückel term at 25 °C. The values of ε (U^{4+}, Cl^-) = 0.76, ε(OH^-, Na^+) = 0.04 were obtained from literature

Table 2
Summary of the thermodynamic constants in the tetravalent actinide (An(IV)) –ISA systems (I = 0).

Species	log $\beta°$, log $K°_{sp}$ [a)]			
	Th(IV)	U(IV)	Np(IV)	Pu(IV)
$An(OH)_4$(am)	−48.0 [24]	−54.5 [15]	−56.7 [15]	−58.33 [15]
$AnOH^{3+}$	12.2 [25]	13.46 [15]	14.55 [15]	14.6 [15]
$An(OH)_2^{2+}$	23.0 [25]		28.35 [15]	28.6 [15]
$An(OH)_3^+$	32.7 [25]			39.7 [15]
$An(OH)_4$(aq)	39.1 [25]	46 [15]	47.7 [15]	47.8 [15]
An(IV)-ISA				
$An(OH)(ISA)^-$	18.5 [9]			
$An(OH)_3$(ISA)(aq)			45.27 [7]	
$An(OH)_3(ISA)_2^-$	38.4 [9]		47.38 [7]	
$An(OH)_4(ISA)^-$	36.5 [6]	50 [11]	51.94 [7]	54.5 [8]
		48.4 ± 0.4 [This work]		50.97 [10]
$An(OH)_4(ISA)_2^{2-}$	44.8 [9]	51.1 [8]	53.8 [7]	58.7 [8]
		50.6 ± 0.1 [This work]		
$An(OH)_5(ISA)^{2-}$				53.08 [10]

a) The literature values for the constants were recalculated using the equations described in the present study.

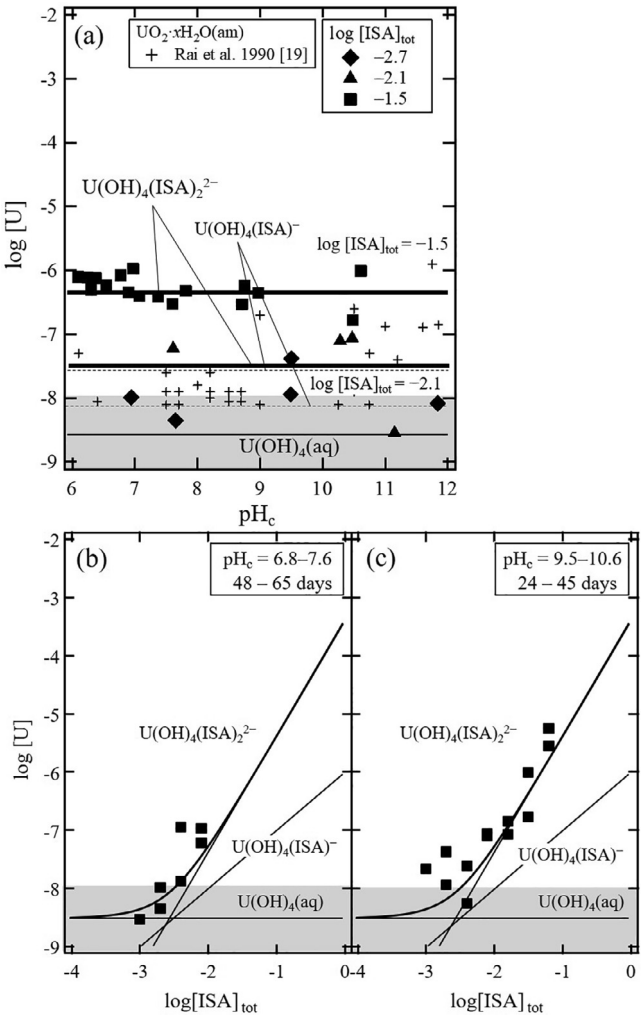


Fig. 7. U(IV) solubility curve and soluble species in the presence of ISA as a function of (a) pH_c and as a function of $[ISA]_{tot}$ at (b) pH_c = 6.8–7.6 and (c) pH_c = 9.5–10.6. The plots show the experimental values, and the solid and bold curves represent the U(IV)-ISA complexes and U(IV) solubility, respectively, calculated from the constants shown in Table 1.

[15] and those of $U(OH)_4(ISA)^-$ and $U(OH)_4(ISA)_2^{2-}$ were estimated to be −0.05 and −0.1, respectively, according to the empirical correction proposed by Hummel et al. [3]. The value of $\varepsilon(CH_3COO^-, Na^+)$ = 0.08 [15] was used for $\varepsilon(ISA^-, Na^+)$ owing to the lack of data. For the hydrolysis species of $U(OH)_m^{(4-m)}$ in Eq. (7), UOH^{3+} and $U(OH)_4(aq)$ were considered and their hydrolysis constants and ion interaction parameters were obtained from literature [15].

Based on Eq. (7), the solubility data in Figs. 2 and 3 were analyzed by least squares fitting analysis, and $\log \beta^\circ_{141}$ and $\log \beta^\circ_{142}$ were determined to be 48.4 ± 0.4 and 50.6 ± 0.1, respectively. The fixed and fitting parameters in the analysis are shown in Table 1 and the formation constants of tetravalent actinide ISA complexes are summarized in Table 2. The complex formation constant for $U(OH)_4(ISA)_2^{2-}$ obtained in the present study ($\log \beta^\circ_{142}$ = 50.6 ± 0.1) was close to the value of $\log \beta^\circ_{142}$ = 51.1, which was estimated from the linear free-energy relationship between the values for other tetravalent actinides [8].

Fig. 7(a) represents the solubility curve and contributions of the ISA complexes in the presence of $10^{-2.1}$ and $10^{-1.5}$ M ISA calculated from the thermodynamic constants in Table 1. In the region of pH_c = 6–12, the U(IV) solubility values were well described by the proposed complexes. Figs. 7(b) and 7(c) show the solubility curve and the contributions of the ISA complexes as a function of $\log [ISA]_{tot}$. It is noteworthy that the experimental plots were well reproduced by $U(OH)_4(ISA)_2^{2-}$ and the contribution of $U(OH)_4(ISA)^-$ was found to be rather limited within the conditions of low ISA concentrations.

3.3.2. Thermodynamic interpretation of U(VI)-ISA system

For the U(VI) system in the region of pH_c = 7–13, the solubility the limiting solid phase was $Na_2U_2O_7{\cdot}H_2O$(cr). In the presence of ISA, the U(VI) solubility was found to be almost constant against pH_c, suggesting that three OH^- ions were involved in the U(VI)-ISA complex. In conjunction with the slope of two of the solubility against $[ISA]_{tot}$, the form of the dominant species can be expressed as $UO_2(OH)_3(ISA)_2^{3-}$. The equilibrium reactions for the solid phase and $UO_2(OH)_3(ISA)_2^{3-}$ are described below.

$$1/2\,Na_2U_2O_7 \cdot H_2O(cr) + H_2O \rightleftharpoons Na^+ + UO_2^{2+} + 3OH^- \quad (11)$$

$$\log K_{sp6} = \log[Na^+] + \log[UO_2^{2+}] + 3\log[OH^-], \quad (12)$$

$$UO_2^{2+} + 3OH^- + ISA^- \rightleftharpoons UO_2(OH)_3(ISA)_2^{3-} \quad (13)$$

$$\log \beta_{132} = \log\left[UO_2(OH)_3(ISA)_2^{3-}\right] - \log\left[UO_2^{2+}\right] - 3\log[OH^-] - 2\log[ISA^-] \quad (14)$$

In addition to the proposed species, the U(VI) hydrolysis species of $(UO_2)_x(OH)_y^{(2x-y)}$ and binary U(VI)-ISA complexes of $UO_2(ISA)_z^{(2-z)}$ were obtained from literature [12,15]. Therefore, the U(VI) solubility ([U(VI)]) as a sum of these species can be described as

Table 3
Summary of thermodynamic constants in U(VI)-ISA system (I = 0).

Reactions		Values	Ref
$1/2Na_2U_2O_7{\cdot}H_2O(s) + H_2O \rightleftharpoons Na^+ + UO_2^{2+} + 3OH^-$	$\log K_{sp6}$	−29.8	[21]
$UO_2^{2+} + OH^- \rightleftharpoons UO_2OH^+$	$\log \beta^\circ_{110}$	8.75	[15]
$UO_2^{2+} + 2OH^- \rightleftharpoons UO_2(OH)_2(aq)$	$\log \beta^\circ_{120}$	15.85	
$UO_2^{2+} + 3OH^- \rightleftharpoons UO_2(OH)_3^-$	$\log \beta^\circ_{130}$	21.75	
$UO_2^{2+} + 4OH^- \rightleftharpoons UO_2(OH)_4^{2-}$	$\log \beta^\circ_{140}$	23.6	
$2UO_2^{2+} + OH^- \rightleftharpoons (UO_2)_2OH^{3+}$	$\log \beta^\circ_{210}$	11.3	
$2UO_2^{2+} + 2OH^- \rightleftharpoons (UO_2)_2(OH)_2^{2+}$	$\log \beta^\circ_{220}$	22.38	
$3UO_2^{2+} + 4OH^- \rightleftharpoons (UO_2)_3(OH)_4^{2+}$	$\log \beta^\circ_{340}$	44.1	
$3UO_2^{2+} + 5OH^- \rightleftharpoons (UO_2)_3(OH)_5^+$	$\log \beta^\circ_{350}$	54.45	
$4UO_2^{2+} + 7OH^- \rightleftharpoons (UO_2)_4(OH)_7^+$	$\log \beta^\circ_{470}$	76.1	
$UO_2^{2+} + ISA^- \rightleftharpoons UO_2ISA^+$	$\log \beta^\circ_{101}$	2.91	[12]
$UO_2^{2+} + 2ISA^- \rightleftharpoons UO_2(ISA)_2(aq)$	$\log \beta^\circ_{102}$	5.37	
$UO_2^{2+} + 3ISA^- \rightleftharpoons UO_2(ISA)_3^-$	$\log \beta^\circ_{103}$	7.25	
$UO_2^{2+} + 3OH^- + 2ISA^- \rightleftharpoons UO_2(OH)_3(ISA)_2^{3-}$	$\log \beta^\circ_{132}$	27.5 ± 0.1	Present study

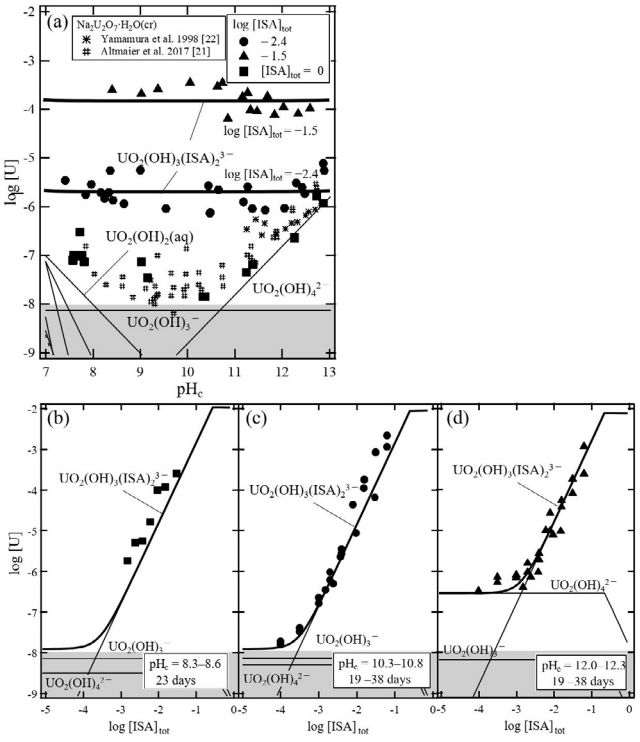


Fig. 8. U(VI) solubility curve and soluble species in the presence of ISA as a function of (a) pH_c and as a function of $[ISA]_{tot}$ at (b) pH_c 8.4 (c) 10.5 and (d) 12.3. The plots exhibit the experimental values, and the solid and bold curves represent the U(VI)-ISA complexes and U(VI) solubility, respectively, calculated from the constants shown in Table 3.

$$[U(VI)] = \left[UO_2^{2+}\right] + \sum_{x,y}\left[(UO_2)_x(OH)_y^{(2x-y)}\right] + \sum_{z}\left[UO_2(ISA)_z^{(2-z)}\right] + \left[UO_2(OH)_3(ISA)_2^{3-}\right] \quad (15)$$

The $[ISA]_{tot}$ was similarly treated as that in the analysis of the U(IV)-ISA system and $[ISA]_{tot} = [ISA^-]$ was assumed. The complex formation constant of $UO_2(OH)_3(ISA)_2^{3-}$ was determined by the least squares fitting analysis of the solubility data shown in Figs. 5 and 6. The fixed and determined parameters in the analysis are summarized in Table 3. Based on the SIT approach, the conditional complex formation constant (β_{132}) for $UO_2(OH)_3(ISA)_2^{3-}$ can be described as

$$\begin{aligned}\log\beta_{132} &= \log\beta^\circ_{132} + \log\gamma_{UO_2(OH)^3(ISA)_2^{3-}} \\ &-\left(\log\gamma_{UO_2^{2+}} + 3\log\gamma_{OH^-} + 2\log\gamma_{ISA^-}\right) \\ &= \log\beta^\circ_{132} - 0\cdot D \\ &-\left\{\varepsilon\left(UO_2(OH)_3(ISA)_2^{3-}, Na^+\right) - \varepsilon\left(UO_2^{2+}, Cl^-\right) - 3\varepsilon(OH^-, Na^+)\right. \\ &\left.-2\varepsilon(ISA^-, Na^+)\right\}\cdot I_m \end{aligned} \quad (16)$$

where β°_{132} is the complex formation constant at $I = 0$. The $\varepsilon\left(UO_2(OH)_3(ISA)_2^{3-}, Na^+\right)$ and $\varepsilon\left(UO_2^{2+}, Cl^-\right)$ represent the ion interaction coefficient for each species. The ion interaction parameter values for UO_2^{2+} and $(UO_2)_x(OH)_y^{(2x-y)}$ were obtained from literature [15] and those for $UO_2(ISA)_z^{(2-z)}$ were assumed to be comparable to those of $(UO_2)_x(OH)_y^{(2x-y)}$ with the same charge. The $\varepsilon\left(UO_2(OH)_3(ISA)_2^{3-}, Na^+\right)$ was assumed to be −0.15 according to the empirical correction proposed by Hummel et al. [3]

Through least squares fitting analysis of the solubility data, $\log\beta^\circ_{132}$ was determined to be 27.5 ± 0.1. Considering that $\log\beta^\circ_{130} = 21.75$ for $UO_2(OH)_3^-$ and $\log\beta^\circ_{102} = 5.37$ for $UO_2(ISA)_2$(aq), $UO_2(OH)_3(ISA)_2^{3-}$ was found to exhibit a large stability constant. The hydroxyl groups on the alkyl chain of ISA may be deprotonated in the investigated pH range to form the stable complex:

$$\begin{aligned} UO_2(OH)_3(ISA)_2^{3-} &\rightleftharpoons UO_2(OH)_2(ISA)(ISA_{-H})^{3-} + H_2O \\ &\rightleftharpoons UO_2(OH)(ISA_{-H})_2^{3-} + 2\ H_2O \end{aligned} \quad (17)$$

The formations of $UO_2(OH)_3(ISA)_2^{3-}$, $UO_2(OH)_2(ISA)(ISA_{-H})^{3-}$, and $UO_2(OH)(ISA_{-H})_2^{3-}$ are compatible with the hydrolysis of UO_2^{2+} and deprotonation of the hydroxyl groups of ISA. The difference between the formations of these species does not appear in the solubility experiment and analysis.

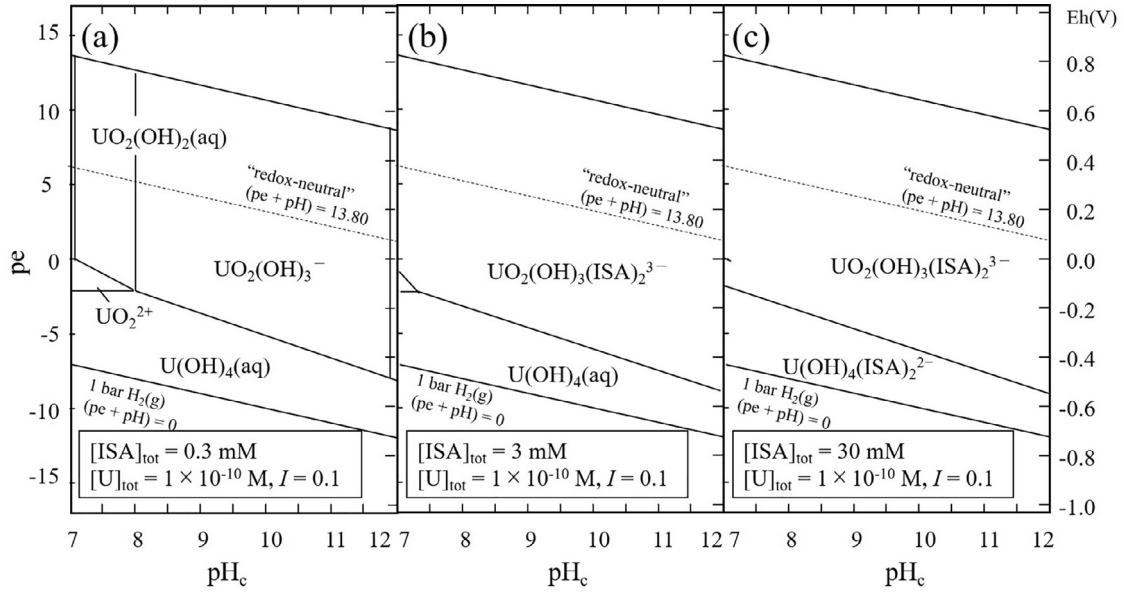


Fig. 9. Pourbaix diagram for U(IV/VI) in the absence and presence of (a) 0.3, (b) 3, and (c) 30 mM ISA at $I = 0.1$ with the total uranium concentration ($[U]_{tot}$) = 10^{-10} M. The represented redox borderlines were calculated based on the thermodynamic constants in Tables 1 and 3. It is noteworthy that the ionic strength correction was performed using the equations by Helgeson et al. [26] within the chemical diagram calculation program by Puigdomenech [27].

Fig. 8 represents the solubility curve in the presence of $10^{-2.4}$ and $10^{-1.5}$ M ISA and the contributions of the ISA complexes, as calculated from the thermodynamic constants in Table 3.

3.3.3. Simulation of uranium(IV/VI) isosaccharinate system

Fig. 9 shows the Pourbaix diagram for U(IV/VI) in the presence of 0.3, 3, and 30 mM ISA at $I = 0.1$ with the total uranium concentration ($[U]_{tot}$) = 10^{-10} M. The represented redox borderlines in the presence of ISA were calculated based on the thermodynamic constants used and obtained in the present study (Tables 1 and 3). The ionic strength was corrected using the equations by Helgeson et al. [26] within the chemical diagram calculation program by Puigdomenech [27]. As shown in Fig. 9(a), the dominant species were U(VI) and U(IV) hydrolysis species in the presence of 0.3 mM ISA, while the dominant U(VI) species was exchanged to $UO_2(OH)_3(ISA)_2^{3-}$ at $[ISA]_{tot} > 3$ mM, and dominant U(IV) species to $U(OH)_4(ISA)_2^{2-}$ at $[ISA]_{tot} > 30$ mM. Comparing the redox borderline of $UO_2(OH)_3^-$ – $U(OH)_4(aq)$ in Fig. 9(a) to that of $UO_2(OH)_3(ISA)_2^{3-}$ – $U(OH)_4(aq)$ in Fig. 9(b), the stability field of U(VI) was slightly expand by the formation of $UO_2(OH)_3(ISA)_2^{3-}$. Meanwhile, no significant difference was observed between the redox borderlines between $UO_2(OH)_3(ISA)_2^{3-}$ – $U(OH)_4(aq)$ in Fig. 9(b) and $UO_2(OH)_3(ISA)_2^{3-}$ – $U(OH)_4(ISA)_2^{2-}$ in Fig. 9(c).

4. Conclusions

In the present study, the effect of ISA on the solubility and redox of U(IV) and U(VI) was investigated as a function of pH_c and $[ISA]_{tot}$. The dependence of U(IV) solubility on the pH_c and $[ISA]_{tot}$ suggested the existence of $U(OH)_4(ISA)_2^{2-}$ as the dominant species in the pH_c range of 6–12. For the U(VI)-ISA system, $UO_2(OH)_3(ISA)_2^{3-}$ was suggested as a dominant species at pH_c 7–13. The formation constants of the U(IV)-ISA and U(VI)-ISA complexes were determined by the least squares fitting analysis of the solubility data. The solubilities of U(IV) and U(VI) in the presence of ISA and their effects on the redox behavior were explained based on the obtained constants.

Acknowledgement

This work was performed as part of the Project on 'The project for validating assessment methodology in geological disposal system (in JFYs 2016 – 2017)' and 'Advanced technology development for geological disposal of TRU waste (in JFY2018)' funded by the Agency for Natural Resources and Energy, Ministry of Economy, Trade and Industry of Japan. This study was partly conducted under the Visiting Researchers Program of the Institute for Integrated Radiation and Nuclear Science, Kyoto University (KURNS).

Appendix A. Supplementary data

Supplementary data to this article can be found online at https://doi.org/10.1016/j.jct.2019.06.006.

References

[1] I. Pavasars, J. Hagberg, H. Borén, B. Allard, Alkaline degradation of cellulose: mechanisms and kinetics, J. Polym. Environ. 11 (2003) 39–47.
[2] C.J. Knill, J.F. Kennedy, Degradation of cellulose under alkaline conditions, Carbohydr. Polym. 51 (2003) 281–300.
[3] W. Hummel, G. Anderegg, L. Rao, I. Puigdomènech, O. Tochiyama, Chemical Thermodynamics 9: Chemical Thermodynamics of Compounds and Complexes of U, Np, Pu, Am, Tc, Se, Ni and Zr with Selected Organic Ligands, NEA OECD. Elsevier, 2005.
[4] B.F. Greenfield, M.H. Hurdus, M.W. Spindler, H.P. Thomason, The Effect of the Products from the Anaerobic Degradation of Cellulose on the Solubility and Sorption of Radioelements in the Near Field Report NSS/R376, UK NIREX, UK, 1997.
[5] A.D. Moreton, N.J. Pilkington, C.J. Tweed, Thermodynamic Modeling of the Effect of Hydroxycarboxylic Acids on the Solubility of Plutonium at High pH Report NSS/R339, UK NIREX, UK, 2000.
[6] K. Vercammen, M.A. Glaus, L.R. Van Loon, Complexation of Th(IV) and Eu(III) by α-isosaccharinic acid under alkaline conditions, Radiochim. Acta 89 (2001) 393–401.
[7] D. Rai, N.J. Hess, Y. Xia, L. Rao, H.M. Cho, R.C. Coore, L.R. Van Loon, Comprehensive thermodynamic model applicable to highly acidic to basic conditions for isosaccharinate reactions with Ca(II) and Np(IV), J. Solution Chem. 32 (2003) 665–689.
[8] X. Gaona, V. Montoya, E. Colas, M. Grive, L. Duro, Review of the complexation of tetravalent actinides by ISA and gluconate under alkaline to hyperalkaline conditions, J. Contaminant Hydrol. 102 (2008) 217–227.
[9] D. Rai, M. Yui, D.A. Moore, L. Rao, Thermodynamic model for ThO_2(am) solubility in isosaccharinate solutions, J. Solution Chem. 382 (2009) 1573–1587.
[10] A. Tasi, X. Gaona, D. Fellhauer, M. Böttle, J. Rothe, K. Dardenne, R. Polly, M. Grivé, E. Colàs, J. Bruno, K. Källström, M. Altmaier, H. Geckeis, Thermodynamic description of the plutonium – α-D-isosaccharinic acid system I: solubility, complexation and redox behavior, Appl. Geochem. 98 (2018) 247–264.
[11] P. Warwick, N. Evans, T. Hall, S. Vines, Stability constants of uranium (IV)-α-isosaccharinic acid and gluconic acid complexes, Radiochim. Acta 92 (2004) 897–902.
[12] L. Rao, A. Garnov, D. Rai, Y. Xia, R. Moore, Protonation and complexation of isosaccarinic acid with U(VI) and Fe(III) in acidic solutions: potentiometric and calorimetric studies, Radiochim. Acta 92 (2004) 575–581.
[13] C.F. Baes, R.E. Mesmer, Hydrolysis of Cations, Wiley, New York, 1976.
[14] I. Grenthe, J. Fuger, R.J.M. Konings, R.J. Lemire, A.B. Müller, C. Nguyen-Trung, H. Wanner, Thermodynamics of uranium, in: F.J. Mompean (Ed.), Chemical Thermodynamics, Elsevier, North-Holland, Amsterdam, 1992.
[15] R. Guillaumont, Th. Fanghänel, J. Fuger, I. Grenthe, V. Neck, D. Palmer, M. Rand, Update on the chemical thermodynamics of Uranium, Neptunium, Plutonium, Americium and Technetium, in: F.J. Mompean (Ed.), Chemical Thermodynamics, Elsevier, North-Holland, Amsterdam, 2003.
[16] R. Whistler, J. Bemiller, α-D-Isosaccharino-1,4-Lactone: Action of Lime Water on Lactose, Methods in Carbohydrate Chemistry Vol. 2: Reactions of Carbohydrates, Academic Press, 1963, pp. 477–479.
[17] T. Kobayashi, T. Teshima, T. Sasaki, A. Kitamura, Thermodynamic model for Zr solubility in the presence of gluconic acid and isosaccharinic acid, J. Nucl. Sci. Technol. 54 (2017) 233–241.
[18] J.L. Ryan, D. Rai, The Solubility of uranium(IV) hydrous oxide in sodium hydroxide solutions under reducing conditions, Polyhedron 2 (1983) 947–952.
[19] D. Rai, A.R. Felmy, J.L. Ryan, Uranium(IV) hydrolysis constants and solubility product of $UO_2{\cdot}xH_2O$, Inorg. Chem. 29 (1990) 260–264.
[20] K. Fujiwara, H. Yamana, T. Fujii, H. Moriyama, Determination of uranium(IV) hydrolysis constants and solubility product of $UO_2{\cdot}xH_2O$, Radiochim. Acta 91 (2003) 345–350.
[21] M. Altmaier, E. Yalcintas, X. Gaona, V. Veck, R. Müller, M. Schlieker, Th. Fanghänel, Solubility of U(VI) in chloride solutions. I. The stable oxides/hydroxides in NaCl systems, solubility products, hydrolysis constants and SIT coefficients, J. Chem. Thermodyn. 114 (2017) 2–13.
[22] T. Yamamura, A. Kitamura, A. Fukui, S. Nishikawa, T. Yamamoto, H. Moriyama, Solubility of U(VI) in Highly Basic Solutions, Radiochim. Acta 83 (1998) 139–146.
[23] D. Rai, A. Kitamura, Evaluation of equilibrium constants for deprotonation and lactonization of α-D-isosaccharinic acid, J. Nucl. Sci. Technol. 53 (2016) 459–467.
[24] T. Kobayashi, T. Sasaki, I. Takagi, H. Moriyama, Solubility of thorium(IV) in the presence of oxalic and malonic acids, J. Nucl. Sci. Technol. 46 (2009) 1085–1090.
[25] T. Sasaki, Y. Takaoka, T. Kobayashi, T. Fujii, I. Takagi, H. Moriyama, Hydrolysis constants and complexation of Th(IV) with carboxylates, Radiochim. Acta 96 (2008) 799–803.
[26] H.C. Helgeson, D.H. Kirkham, G.C. Flowers, Theoretical prediction of the thermodynamic behavior of aqueous electrolytes by high pressures and temperatures; IV, Calculation of activity coefficients, osmotic coefficients, and apparent molal and standard and relative partial molal properties to 600 degrees C and 5kb, Am. J. Sci. 281 (1981) 1249–1516.
[27] I. Puigdomenech, "HYDRA (Hydrochemical Equilibrium- Constant Database) and MEDUSA (Make Equilibrium Diagrams Using Sophisticated Algorithms) Programs," Royal Institute of Technology, Sweden. http://www.ke- mi.kth.se/medusa.